Journal of Organometallic Chemistry, 383 (1990) 421–440
Elsevier Sequoia S.A., Lausanne – Printed in The Netherlands
JOM 20238

Syntheses and structures of rhodium-osmium clusters derived from the reaction of $(\mu\text{-H})_2Os_3(CO)_{10}$ with $(\eta^5\text{-}C_5H_5)Rh(CO)_2$

Anne Colombie *, **Deborah A. McCarthy, Jeanette Krause, Leh-Yeh Hsu, Wen-Liang Hsu, Deng-Yang Jan, and Sheldon G. Shore** *

Department of Chemistry, The Ohio State University, Columbus, Ohio 43210 (U.S.A.)

(Received April 19th, 1989)

Abstract

The reaction between $(\mu\text{-H})_2Os_3(CO)_{10}$ and $(\eta^5\text{-}C_5H_5)Rh(CO)_2$ in toluene at 90 °C produces $(\eta^5\text{-}C_5H_5)RhOs_2(CO)_9$ (I) and $(\mu\text{-H})_2(\eta^5\text{-}C_5H_5)RhOs_3(CO)_{10}$ (II), as the principal products while the pentanuclear cluster $(\mu\text{-H})_2(\eta^5\text{-}C_5H_5)RhOs_4(CO)_{13}$ (III) is obtained in low yield. When added hydrogen is present during the reaction, replacement of the cyclopentadienide ligand by toluene occurs and the principal product is $(\mu\text{-H})_3(\eta^6\text{-}C_6H_5CH_3)RhOs_3(CO)_9$ (VI). Also produced in this reaction are $(\mu\text{-H})_2(\eta^5\text{-}C_5H_5)_2Rh_2Os_2(CO)_7$ (IV) and cluster II, but in low yields. In benzene in the presence of H_2, an analogous reaction occurs. The cyclopentadienide ligand is replaced by benzene to give $(\mu\text{-H})_3(\eta^6\text{-}C_6H_6)RhOs_3(CO)_9$ (VII) as the main product and clusters II and $(\mu\text{-H})_4(\eta^5\text{-}C_5H_5)RhOs_3(CO)_9$ (V) are formed in small yields. Conversion of clusters I and II to clusters IV and V, respectively, was achieved by bubbling H_2 through toluene solutions of I and II at 90 °C. Cluster V is moderately unstable in solution, with significant decomposition occurring during the reaction. The molecular structures of clusters II, III, IV, and VII have been determined by single crystal X-ray diffraction studies. Clusters II, IV, and VII have tetrahedral metal cores, while the pentanuclear cluster III has an Os tetrahedral core which is edge bridged by a Rh atom. For compound II: space group $P2_1/n$, a 8.120(3), b 14.932(3), c 16.277(3) Å, β 91.29(4)°, V 1972.9 Å^3, $Z = 4$, mol wt = 1020.73, ρ_{calcd} 3.434 gm cm^{-3}, and μ_{calcd} 201.5 cm^{-1} for Mo-K_α; 3885 independent reflections $\geq 3\sigma(I)$; $4 \leq 2\theta \leq 55°$ obtained at −35 °C; final R_f 5.7%, R_{wf} 7.4%. For compound III: space group $P2_1/c$, a 11.134(2), b 16.649(2), c 14.015(2) Å, β 109.98(1)°, V 2441.6 Å^3, $Z = 4$, mol wt = 1294.95, $\rho_{\text{calcd}} = 2.773$ gm cm^{-3}, and μ_{calcd} 162.6 cm^{-1} for Mo-K_α; 5695 independent reflections $\geq 3\sigma(I)$; $4 \leq 2\theta \leq 50°$ at −30 °C; final R_f 2.95%, R_{wf} 4.0%. For compound IV: space group $P2_1/c$, a 8.186(3), b 15.651(5), c 15.723(2) Å, β 97.32°, V 1998.25 Å^3, $Z = 4$,

---

* Deceased.

0022-328X/90/$03.50

mol wt = 914.49, ρ_{calcd} 3.038 gm cm^{-3}, and μ_{calcd} 143.34 cm^{-1} for Mo-K_α; 3619 independent reflections $\geqslant 3\sigma(I)$; $4 \leqslant 2\theta \leqslant 55°$ at 25°C; final R_f 3.3%, R_{wf} 4.5%. For compound VII: space group $R\bar{3}$, $a = b = c = 10.003(4)$ Å, $\alpha = \beta = \gamma = 92.16(3)°$, $V = 998.3$ Å^3, $Z = 2$, mol wt = 1006.5, ρ_{calcd} 3.34 gm cm^{-3}, and μ_{calcd} 214.8 cm^{-1} Mo-K_α; 3017 independent reflections $\geqslant 3\sigma(I)$; $4 \leqslant 2\theta \leqslant 50°$ at 25°C; Final R_f 4.4%, R_{wf} 6.3%.

Introduction

A number of studies in this and other laboratories have focused on the use of $(\mu\text{-H})_2Os_3(CO)_{10}$ as the starting material for triosmium based mixed metal clusters [1–12]. Reaction of $(\mu\text{-H})_2Os_3(CO)_{10}$ with carbonyls of the first row transition metals has led to the formation of a variety of clusters. In our studies of first row metal carbonyls, tetranuclear clusters with MOs_3 (M = Fe, Co, Ni) metal cores were the only products identified [1–3a]. We found that the product composition and distribution was dependent upon the absence or presence of added H_2 during the reactions studied. In the absence of added H_2, the only product was $(\mu\text{-H})_2(\eta^5\text{-}C_5H_5)MOs_3(CO)_{10}$ (M = Co, Ni) [3a]. In the presence of added H_2 this cluster was produced in low yield and the principal products were $(\mu\text{-H})_3(\eta^5\text{-}C_5H_5)MOs_3(CO)_9$ (M = Co, Ni) and $(\mu\text{-H})_4(\eta^5\text{-}C_5H_5)MOs_3(CO)_9$ (M = Co).

This type of reaction, in the absence and presence of added hydrogen, was extended to carbonyls of the second row transition metals. We found that clusters with trinuclear MOs_2 (M = Rh) [5,6], tetranuclear MOs_3 (M = Mo, Rh) [5,6,10–12], M_2Os_2 (M = Rh) [10], and pentanuclear M_2Os_3 (M = Mo) [11] cores were produced. When the pentamethylcyclopentadienide complexes $[(\eta^5\text{-}C_5(CH_3)_5Rh(CO)]_2$ and $(\eta^5\text{-}C_5(CH_3)_5)Rh(CO)_2$ were allowed to react with $(\mu\text{-H})_2Os_3(CO)_{10}$ [10] in the absence of added hydrogen, the products were $(\mu\text{-H})_2(\eta^5\text{-}C_5(CH_3)_5)RhOs_3(CO)_{10}$, $(\mu\text{-H})_2(\eta^5\text{-}C_5(CH_3)_5)_2Rh_2Os_2(CO)_7$, and $(\eta^5\text{-}C_5(CH_3)_5)_2Rh_2Os_2(CO)_8$. In the presence of added H_2, $(\mu\text{-H})_2(\eta^5\text{-}C_5(CH_3)_5)_2Rh_2Os_2(CO)_7$ and $(\mu\text{-H})_4(\eta^5\text{-}C_5(CH_3)_5)RhOs_3(CO)_9$ were formed. In a similar reaction of $Ru_3(CO)_{12}$ with $(\eta^5\text{-}C_5H_5)Rh(CO)_2$ in the presence of H_2 in octane Lindsell, Knobler, and Kaesz [13] obtained $(\mu\text{-H})_2(\eta^5\text{-}C_5H_5)RhRu_3(CO)_{10}$, an analogue of $(\mu\text{-H})_2(\eta^5\text{-}C_5H_5)RhOs_3(CO)_{10}$ as the principal product.

Earlier results from this laboratory indicated some significant differences between reactions of $(\eta^5\text{-}C_5H_5)Rh(CO)_2$ and $(\eta^5\text{-}C_5(CH_3)_5)Rh(CO)_2$ with $(\mu\text{-H})_2Os_3(CO)_{10}$ with respect to yields of analogous products and product types [5,6,10]. In the present study we have investigated reactions of $(\eta^5\text{-}C_5H_5)Rh(CO)_2$ with $(\mu\text{-H})_2Os_3(CO)_{10}$ in additional detail in order to obtain a more complete view of the dependence of products on the type of cyclopentadienide ligand bound to rhodium.

Experimental

All reactions were run on a vacuum line using standard techniques [14]. Air and moisture sensitive compounds were weighed out under N_2 in a Vacuum Atmospheres glovebox. TLC separations were carried out in air, as all of the neutral products are air and moisture stable.

Chemicals and solvents. Triosmium dodecacarbonyl (Strem), rhodium trichloride hydrate (Aldrich), cyclopentadiene (Aldrich), and prepurified hydrogen (AGA) were used without further purification. Toluene, diethyl ether, and tetrahydrofuran (Mallinckrodt) and their deuterated analogs (ICN, Biomedicals Inc.) were dried by having them refluxed and storing them over sodium benzophenone ketyl. Dried methylene chloride (Mallinckrodt) was distilled from P_2O_5 or CaH_2 and stored under vacuum. $(\mu\text{-}H)_2Os_3(CO)_{10}$ [15] and $[Rh(CO)_2Cl]_2$ [16] were prepared according to published methods.

Infrared and NMR spectra. Infrared spectra of solutions were recorded on a Matteson Cygnus-25 FTIR Spectrometer. Proton and carbon-13 spectra were obtained on a Bruker-300 or Bruker-250 spectrometer at 300.13 or 250.13 MHz respectively. Chemical shifts are referred to $Si(CH_3)_4$ (^1H NMR, δ 0.00 ppm) and $Si(^{13}CH_3)_4$(^{13}C, δ 0.00 ppm).

Mass spectra. Mass spectra were obtained at The Ohio State University Chemical Instrument Center, by use of a Kratos MS-30 (or VG 70-250S) mass spectrometer.

X-ray structure determinations. For X-ray examination and data collection, each crystal was mounted on the tip of a glass fiber. All X-ray data were collected on an Enraf–Nonius CAD4 diffractometer with graphite-monochromated Mo-K_α radiation. All crystallographic computations were carried out on a PDP 11/44 computer using SDP (Structure Determination Package) [17]. Table 1 gives crystallographic data for $(\mu\text{-}H)_2(\eta^5\text{-}C_5H_5)RhOs_3(CO)_{10}$ (II), $(\mu\text{-}H)_2(\eta^5\text{-}C_5H_5)RhOs_4(CO)_{13}$ (III), $(\mu\text{-}H)_2(\eta^5\text{-}C_5H_5)_2Rh_2Os_2(CO)_7$ (IV), and $(\mu\text{-}H)_3(\eta^6\text{-}C_6H_6)RhOs_3(CO)_9$ (VII).

Unit cell parameters for each crystal were obtained by least squares refinement of the angular settings from 25 reflections, well-distributed in reciprocal space and lying in a 2θ range of 24–30°. Intensity data were collected in the ω–2θ scan mode. Six standard reflections were monitored and showed no significant decay. Data were corrected for Lorentz and polarization effects. The intensities were also corrected for absorption effects by applying an empirical method based on the crystal orientation and measured psi scans.

Structures were solved by a combination of the direct method MULTAN 11/82 and the difference Fourier technique, and were refined by full-matrix least squares. Analytical atomic scattering factors were used throughout the structure refinement with both the real and imaginary components of the anomalous dispersion included. The heavy atoms first appeared on the *E*-map. Then the positions of the carbon and oxygen atoms were determined from a Fourier synthesis which was phased on the metal atoms. Full-matrix least squares refinements were carried out using anisotropic thermal parameters for non-hydrogen atoms. Final atomic positional parameters for located atoms are given in Tables 2–5. Positions of hydrogen atoms on the cyclopentadienyl and benzene rings were calculated (d(C–H) 0.95 Å) with their thermal parameters fixed and incorporated into the final three cycles of refinement. Molecular structures are given in Figures 1–3, 5.

Preparation of $(\eta^5\text{-}C_5H_5)Rh(CO)_2$. $(\eta^5\text{-}C_5H_5)Rh(CO)_2$ was prepared by a modification of a method of Fischer and Bittler [18]. In a typical reaction $[Rh(CO)_2Cl]_2$ (1.0 g, 2.5 mmol) was weighed in air and charged to a 50 ml flask. $K[C_5H_5]$ (0.60 g, 5.8 mmol) was weighed in a glovebox and added to the flask. The flask was sealed, evacuated under high vacuum and diethylether (15 ml) was condensed into the flask at −78°C. The solution was warmed to ambient temperature and stirred for 4 h.

Table 1

Crystal data

Chemical formula	$C_{15}H_7O_{10}Os_3Rh$ (II)	$C_{18}H_7O_{13}Os_4Rh$ (III)	$C_{17}H_{12}O_7Os_2Rh_2$ (IV)	$C_{15}H_9O_9Os_3Rh$ (VII)
Mol. wt.	1020.7	1295.0	914.5	1006.5
Color of crystal	dark red	purple	black	yellow
Space group	$P2_1/n$	$P2_1/c$	$P2_1/c$	$R\bar{3}$
Z	4	4	4	2
Temp. (°C)	−35	−30	25	25
a, Å	8.120(3)	11.134(2)	8.186(3)	10.003(4)
b, Å	14.932(3)	16.649(2)	15.651(5)	10.003(4)
c, Å	16.277(3)	14.015(2)	15.723(2)	10.003(4)
α, deg	90.00	90.00	90.00	92.16(3)
β, deg	91.29(4)	109.98(1)	97.32(2)	92.16(3)
γ, deg	90.00	90.00	90.00	92.16(3)
V, Å^3	1972.9	2441.6	1998.3	998.3
ρ(calcd), g cm^{-3}	3.434	2.773	3.038	4.013
μ, cm^{-1}	201.5	214.9	143.2	199.1
Max. trans. %	99.5	99.8	99.6	99.9
Min. trans. %	9.54	55.5	54.7	33.4
Scan mode	$\omega-2\theta$	$\omega-2\theta$	$\omega-2\theta$	$\omega-2\theta$
Radiation (λ, Å)	Mo-K_α (0.710730)	Mo-K_α (0.710730)	Mo-K_α (0.710730)	Mo-K_α (0.710730)
Data collection limits (2θ)	4–55	4–50	4–55	4–50
No. of unique reflections	4619	8198	5062	4812
No. of reflections used in structure refinement ($\geqslant 3\sigma(I)$)	3885	5695	3619	3017
$R_f = \sigma \| \|F_o\| - \|F_c\| \| / \Sigma \|F_o\|$	0.057	0.029	0.033	0.044
$R_{wf} = (\Sigma w(\|F_o\| - \|F_c\|)^2 / \Sigma w \|F_o\|^2)^{1/2}$	0.074	0.040	0.046	0.063
Weighting scheme, $w = [\sigma(I)^2 + (KI)^2]^{-1/2}$	0.04	0.05	0.05	0.03

Diethyl ether was removed by means of rotary evaporation leaving a brown oily residue in the flask. $(\eta^5\text{-}C_5H_5)Rh(CO)_2$ was vacuum distilled from the residue and trapped at −78 °C. $(\eta^5\text{-}C_5H_5)Rh(CO)_2$ is an orange-red mildly air and light sensitive liquid at room temperature.

Reaction of $(\mu\text{-}H)_2Os_3(CO)_{10}$ with $(\eta^5\text{-}C_5H_5)Rh(CO)_2$ in the absence of added hydrogen. In a typical reaction $(\mu\text{-}H)_2Os_3(CO)_{10}$ (130 mg, 0.15 mmol) was added to $(\eta^5\text{-}C_5H_5)Rh(CO)_2$ (100 mg, 0.45 mmol) in a 50 ml flask and sealed with a vacuum adapter. Toluene (ca. 15 ml) was condensed into the flask at −78 °C. After warming the flask to room temperature it was placed in a 90 °C bath and stirred for 3 days. The toluene was removed by means of rotary evaporation leaving a reddish brown solid in the flask. Complete separation of the clusters was accomplished by means of thin layer chromotography on 2-mm silica plates with a mixed solvent, 1/4 toluene/heptane, eluent. This yielded four bands, orange (R_f 0.66), green (R_f 0.33), pink (R_f 0.27) and brown (R_f 0.10).

The orange and green bands were $(\eta^5\text{-}C_5H_5)RhOs_2(CO)_9$ (I) and $(\mu\text{-}H)_2(\eta^5\text{-}C_5H_5)RhOs_3(CO)_{10}$ (II) clusters which were previously identified in this laboratory and reported [5]. Yields: 55 mg, 0.068 mmol, 45%; 60 mg, 0.058 mmol, 42%, based on $(\mu\text{-}H)_2Os_3(CO)_{10}$, for clusters I and II, respectively. Crystals of II for single crystal X-ray analysis were obtained by slow evaporation of solvent from a CH_2Cl_2 solution at room temperature.

Crystals from the pink band were grown from CH_2Cl_2/heptane (layered) at room temperature and were shown to be the new cluster $(\mu\text{-}H)_2(\eta^5\text{-}C_5H_5)RhOs_4(CO)_{13}$ (III), from a single crystal X-ray structure determination. Yield: 5 mg, 4 μmol, 3.5% based on $(\mu\text{-}H)_2Os_3(CO)_{10}$. IR spectrum: ((cyclohexane, ν(CO)) 2090 m, 2055 s, 2039 vs, 2019 s, 2006 w, 2000 m, 1990 w, 1973 m cm^{-1}). ^1H NMR spectrum: (25 °C ($CDCl_3$) 6.04 (s, 5H), −18.24 (s, 2H) ppm). Mass spectrum parent ion peak m/z calcd. for $^{192}Os_4{}^{103}Rh_1{}^{16}O_{13}{}^{12}C_{18}{}^1H_7$: 1302; found: 1300.

The brown band consisted of $(\mu_3\text{-}H)(\mu_3,\ \eta^5\text{-}C_5H_5)(\eta^5\text{-}C_5H_5)_3Rh_3$ [19], which was identified by its ^1H NMR spectrum and a mixture of unidentified products.

Reaction of $(\mu\text{-}H)_2Os_3(CO)_{10}$ with $(\eta^5\text{-}C_5H_5)Rh(CO)_2$ in the presence of added hydrogen. In a typical reaction, H_2 was bubbled through a 20 ml toluene solution of $(\mu\text{-}H)_2Os_3(CO)_{10}$ (105 mg, 0.123 mmol) and $(\eta^5\text{-}C_5H_5)Rh(CO)_2$ (73.6 mg, 0.33 mmol) at ambient temperature for 20 minutes in a 50 ml two-neck flask equipped with a reflux condenser. The solution was then heated to 90 °C for 72 h with continued bubbling of H_2. After cooling the flask to room temperature the volatiles were removed under high vacuum leaving a brown solid. The products were separated by TLC on 2-mm silica with a 1/4 toluene/heptane eluent. This gave three bands, red-orange (R_f 0.43), green (R_f 0.30) and brown (R_f 0.09).

The red-orange band was $(\mu\text{-}H)_2(\eta^6\text{-}C_6H_5CH_3)RhOs_3(CO)_9$ (VI), a cluster previously identified and reported from this laboratory [6]. Yield: 31.5 mg, 0.030 mmol, 25% based on $(\mu\text{-}H)_2Os_3(CO)_{10}$.

The green band was identified from NMR and IR spectra as the previously reported cluster $(\mu\text{-}H)_2(\eta^5\text{-}C_5H_5)RhOs_3(CO)_{10}$ (II) [5]. Yield: 10.1 mg, 0.010 mmol, 8% based on $(\mu\text{-}H)_2Os_3(CO)_{10}$.

The brown band was identified as $(\mu\text{-}H)_2(\eta^5\text{-}C_5H_5)_2Rh_2Os_2(CO)_7$ (IV) from a single crystal X-ray structure analysis. Yield: 6.2 mg, 7 μmol, 7% based on $(\mu\text{-}H)_2Os_3(CO)_{10}$. Single crystals were grown by slow evaporation of hexane into a CH_2Cl_2/hexane solution of the compound. IR spectrum: (cyclohexane, ν(CO))

2072 m, 2044 s, 2001 m, 1990 s, 1971 m, 1958 m, 1806 m cm^{-1}). ^{1}H NMR spectrum: (25 °C ($CDCl_3$) 5.59 (s, 10H), −11.09 (s, 2H) ppm). Mass spectrum parent ion peak *m/z* calcd. for $^{192}Os_2{}^{103}Rh_2{}^{16}O_7{}^{12}C_{17}{}^{1}H_{12}$: 918; Found 918.

Preparation of $(\mu\text{-}H)_3(\eta^6\text{-}C_6H_6)RhOs_3(CO)_9$ *(VII).* This compound was prepared by the same method as compound VI except that the reaction was carried out in benzene at 60 °C. In a typical reaction H_2 was bubbled through a benzene solution (ca. 15 ml) of $(\mu\text{-}H)_2Os_3(CO)_{10}$ (111.2 mg, 0.130 mmol) and $(\eta^5\text{-}C_5H_5)Rh(CO)_2$ (76.9 mg, 0.343 mmol) in a 25 ml two-neck round bottom flask at 60 °C for 72 h. The volatiles were removed under high vacuum leaving a brown solid. Separation by TLC on 2-mm silica, using 1/4 benzene/hexanes as eluent, yielded three bands: orange-red, yellow-green, and brown. Crystals from the orange-red band were grown by slow evaporation of hexane into a CH_2Cl_2/hexane solution and were shown to be $(\mu\text{-}H)_3(\eta^6\text{-}C_6H_6)RhOs_3(CO)_9$ (VII) from a single crystal X-ray analysis. Yield: 13.1 mg, 0.013 mmol, 10% based on $(\mu\text{-}H)_2Os_3(CO)_{10}$. IR spectrum: ((hexanes, ν(CO)) 2070 w, 2048 s, 1994 vs, 1978 m, 1945 vw cm^{-1}). ^{1}H NMR spectrum: (−60 °C (acetone-d_6) 6.68 (s, 6H), −17.43 (s, 3H) ppm). ^{13}C NMR spectrum: (−60 °C (CD_2Cl_2) 176.9 (s, 3C), 172.1 (d, *J* 9 Hz, 9 C) ppm). Mass spectrum parent ion peak *m/z* calcd. for $^{192}Os_3{}^{103}Rh_1{}^{16}O_9{}^{12}C_{15}{}^{1}H_9$: 1012; Found 1012.

The yellow-green band was found to be a mixture of V and II identified by their characteristic ^{1}H NMR peaks. These were present in low yield and were not separated. The brown band consisted of a mixture of low yield unidentified products and $(\mu\text{-}H)_2Os_5(CO)_{16}$ identified by ^{1}H NMR.

Preparation of $(\mu\text{-}H)_2(\eta^5\text{-}C_5H_5)RhOs_3(CO)_{10}$ *(II) and* $(\mu\text{-}H)_2(\eta^5\text{-}C_5H_5)_2Rh_2Os_2(CO)_7$ *(IV) from* $(\eta^5\text{-}C_5H_5)RhOs_2(CO)_9$ *(I).* Hydrogen was bubbled through a 10 ml toluene solution of $(\eta^5\text{-}C_5H_5)RhOs_2(CO)_9$ (21.5 mg, 0.027 mmol) for 40 min at room temperature in a 30 ml two-neck flask equipped with a reflux condenser. Then, with continued bubbling of H_2 through the solution, it was heated to 90 °C for 8 h. The reaction was cooled and the volatiles were removed by means of rotary evaporation. Separation of the products was carried out by TLC with 1/4 benzene/hexane as eluent, giving three bands. They were, an unknown purple solid (trace amounts), green $(\mu\text{-}H)_2(\eta^5\text{-}C_5H_5)RhOs_3(CO)_{10}$ (II) (Yield: 0.7 mg, 0.7 μmol, 5% based on $(\eta^5\text{-}C_5H_5)RhOs_2(CO)_9$ and brown $(\mu\text{-}H)_2(\eta^5\text{-}C_5H_5)_2Rh_2Os_2(CO)_7$ (IV) (Yield: 0.7 mg, 0.8 μmol, 7% based on $(\eta^5\text{-}C_5H_5)RhOs_2(CO)_9$.

Preparation of $(\mu\text{-}H)_4(\eta^5\text{-}C_5H_5)RhOs_3(CO)_9$ *(V) from* $(\mu\text{-}H)_2(\eta^5\text{-}C_5H_5)RhOs_3(CO)_{10}$ *(II).* H_2 was rapidly bubbled for 10 min at room temperature through a toluene solution of $(\mu\text{-}H)_2(\eta^5\text{-}C_5H_5)RhOs_3(CO)_{10}$ (56.9 mg, 0.056 mmol) in a 50 ml two-neck flask equipped with a reflux condenser. The solution was then heated to 90 °C and the hydrogen flow reduced to a moderate rate. The reaction was stirred for 48 h. After cooling the flask to room temperature, the volatiles were removed under high vacuum leaving a dark brown solid in the flask. The solid was dissolved in 0.5 ml of CH_2Cl_2 and separated by TLC on 2-mm silica with 1/4 benzene/hexanes as eluent. This gave a dark yellow band (R_f 0.69), a green band (R_f 0.53), a pink band (R_f 0.21) and a brown band (R_f 0.12). The pink and brown bands were present in only trace quantities and were not identified. The green band was identified as unreacted II, while the dark yellow band was identified as $(\mu\text{-}H)_4(\eta^5\text{-}C_5H_5)RhOs_3(CO)_9$ (V) (Yield: 31 mg, 0.031 mol, 56% based on $(\mu\text{-}H)_2(\eta^5\text{-}C_5H_5)RhOs_3(CO)_{10}$) by IR and NMR spectroscopic comparisons to the known pentamethylcyclopentadiene analogue [10]. IR spectrum: (hexanes, ν(CO)) 2091 w, 2067 s, 2054 vs, 2012 m, 1996 s, 1983 w). ^{1}H NMR ($-80\,^\circ$C ($CDCl_3$) 5.71 (s, 5 H), -18.13 (d, J(Rh–H) $= 25$ Hz, 2 H), -19.47 (s, 2 H) ppm). Mass spectrum parent ion peak m/z calcd. for $^{192}Os_3{}^{103}Rh_1{}^{16}O_9{}^{12}C_{14}{}^1H_9$: 1000; Found 1000. Anal. Found: C, 16.74, H, 0.89. $C_{14}H_9O_9RhOs_3$ calcd.: C, 16.91; H, 0.91%.

Results and discussion

Reaction of (μ-H)$_2$Os$_3$(CO)$_{10}$ with (η^5-C$_5$H$_5$)Rh(CO)$_2$ in the absence and in the presence of added hydrogen. The reaction of (μ-H)$_2$Os$_3$(CO)$_{10}$ with (η^5-C$_5$H$_5$)Rh(CO)$_2$ results in the production of a number of mixed metal clusters whose compositions and yields depend upon the absence or presence of added H_2 and on the solvent used in the reaction. Results are summarized in Scheme 1. When the reaction (1a, Scheme 1) was carried out in toluene in the absence of added H_2, three major products, (η^5-C$_5$H$_5$)RhOs$_2$(CO)$_9$ (I), (μ-H)$_2$(η^5-C$_5$H$_5$)RhOs$_3$(CO)$_{10}$ (II), and (μ-H)$_2$(η^5-C$_5$H$_5$)RhOs$_4$(CO)$_{13}$ (III) were isolated and characterized.

Significantly different products were obtained when additional H_2 was present during the reaction of (μ-H)$_2$Os$_3$(CO)$_{10}$ with (η^5-C$_5$H$_5$)Rh(CO)$_2$ (reaction 1b, Scheme 1). The three major products were (μ-H)$_2$(η^5-C$_5$H$_5$)RhOs$_3$(CO)$_{10}$ (II), (μ-H)$_2$(η^5-C$_5$H$_5$)$_2$Rh$_2$Os$_2$(CO)$_7$ (IV) and (μ-H)$_3$(η^6-C$_6$H$_5$CH$_3$)RhOs$_3$(CO)$_9$ (VI).

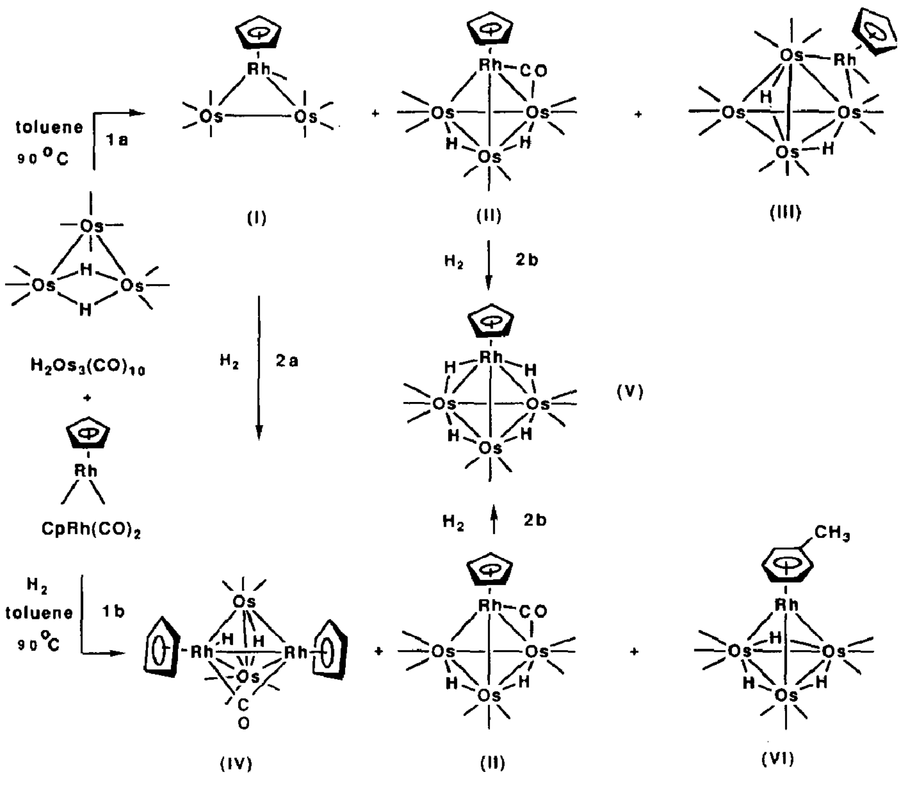

Scheme 1

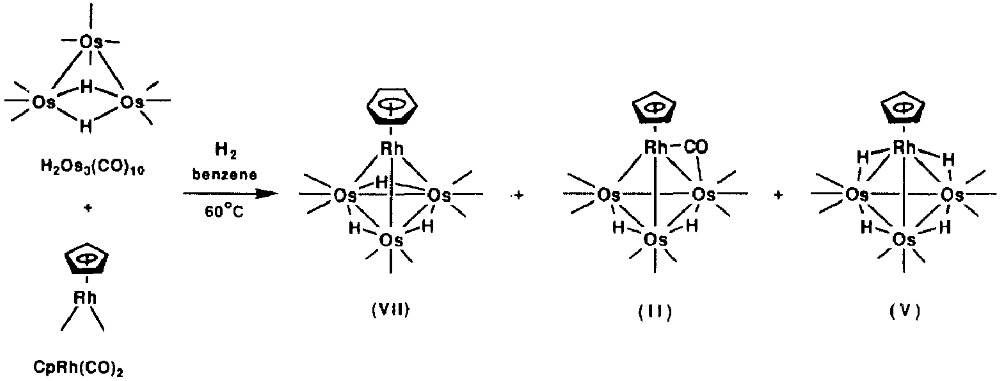

Scheme 2

When the reaction was carried out in benzene in the presence of added H_2 the major product was $(\mu\text{-H})_3(\eta^6\text{-}C_6H_6)RhOs_3(CO)_9$ (VII) (Scheme 2).

These products differ with respect to product types or yields from those obtained from analogous reactions which employed the pentamethylcyclopentadienyl derivative, $(\eta^5\text{-}C_5(CH_3)_5)Rh(CO)_2$ [10]. In the absence of added H_2 the products were $(\eta^5\text{-}C_5(CH_3)_5)_2Rh_2Os_2(CO)_8$, $(\mu\text{-H})_2(\eta^5\text{-}C_5(CH_3)_5)RhOs_3(CO)_{10}$ and $(\mu\text{-H})_2(\eta^5\text{-}C_5(CH)_3)_2Rh_2Os_2(CO)_7$. In the presence of added H_2 the products were $(\mu\text{-H})_4(\eta^5\text{-}C_5(CH_3)_5)RhOs_3(CO)_9$ and $(\mu\text{-H})_2(\eta^5\text{-}C_5(CH_3)_5)Rh_2Os_2(CO)_7$.

Added H_2 is required for the formation of clusters $(\mu\text{-H})_3(\eta^6\text{-}C_6H_5CH_3)RhOs_3(CO)_9$ (VI) and $(\mu\text{-H})_3(\eta^6\text{-}C_6H_6)RhOs_3(CO)_9$ (VII) products which contain toluene and benzene, respectively, in place of the cyclopentadienyl ligand in the starting complex, $(\eta^5\text{-}C_5H_5)Rh(CO)_2$. Such substitution did not occur when the starting material contained the pentamethylcyclopentadienyl ligand $(\eta^5\text{-}C_5(CH_3)_5)Rh(CO)_2$ [10]. The requirement that H_2 be present for the substitution reaction to occur suggests that the cyclopentadienyl ligand attached to rhodium is effectively hydrogenated to yield cyclopentadiene or cyclopentane which is replaced by the toluene or benzene. It seems likely that hydrogen reacts oxidatively with the starting material, $(\eta^5\text{-}C_5H_5)Rh(CO)_2$, and then reduces the cyclopentadienyl which then may be eliminated as cyclopentadiene or cyclopentane with addition of the arene to the rhodium. This possibility is supported by the recent report by Maitlis [20] of elimination of pentamethylcyclopentadiene from the hydrido compound $(\eta^5\text{-}C_5(CH_3)_5)RhH_3(SiEt_3)$ and its replacement by trimethyl phosphine. We were unable to isolate any likely intermediate species when the starting material $(\eta^5\text{-}C_5H_5)Rh(CO)_2$ was treated with H_2 in toluene under conditions required to form VI.

Since the yield of $(\mu\text{-H})_2(\eta^5\text{-}C_5H_5)RhOs_3(CO)_{10}$ (II) is significantly smaller when added H_2 is present in the reaction (reaction 1b, Scheme 1), the possibility was also considered that the η^6-substituted products VI and VII can be formed by the hydrogenation of the cyclopentadienide ligand on cluster II, accompanied by reaction with the toluene or benzene solvent. To test this possibility we examined the reaction of $(\mu\text{-H})_2(\eta^5\text{-}C_5H_5)RhOs_3(CO)_{10}$ (II) with H_2 in toluene under conditions similar to those under which VI was formed (reaction 2b, Scheme 1). This reaction produced the cluster $(\mu\text{-H})_4(\eta^5\text{-}C_5H_5)RhOs_3(CO)_9$ (V). There was no indication for the formation of $(\mu\text{-H})_2(\eta^6\text{-}C_6H_5CH_3)RhOs_3(CO)_9$ (VI). In principle, cluster V could be converted to VI in toluene by the transfer of a hydrogen atom to the cyclopentadienyl ligand with elimination of cyclopentadiene and CO in the formation of the η^6-$C_6H_5CH_3$ complex. However, since no VI was observed as a product in the reaction in which V is formed in significant yield (56%) this is an unlikely pathway to VI under normal reaction conditions.

The presence of added H_2 is required for the formation of $(\mu$-$H)_4(\eta^5$-$C_5H_5)RhOs_9(CO)_9$ (V) (reaction 2b, Scheme 1). The absence of V as a product from reaction 1b, Scheme 1 and the relatively low yield of $(\mu$-$H)_2(\eta^5$-$C_5H_5)RhOs_3(CO)_9$ (II) compared to that of $(\mu$-$H)_3(\eta^6$-$C_6H_5CH_3)RhOs_3(CO)_9$ (VI), implies that II and VI are formed through competing reactions and that replacement of the cyclopentadienide ligand by toluene predominates. Since VI is not formed from II or V and since there is no evidence of toluene substituting for cyclopentadienide ligand on the starting rhodium complex, the pathway to VI undoubtedly requires an intermediate hydridorhodium species which has not been identified.

The presence of H_2 is also required for the formation of $(\mu$-$H)_2(\eta^5$-$C_5H_5)_2Rh_2Os_2(CO)_7$ (IV), a cluster with an Rh_2Os_2 core. In the analogous reactions with the pentamethylcyclopentadienyl derivative, $(\eta^5$-$C_5(CH_3)_5)Rh(CO)_2$, Rh_2Os_2 core clusters are the favored products [10]. It has been proposed that under the reaction conditions employed, monomeric rhodium starting material slowly forms a dimer which then goes on to form the Rh_2Os_2 mixed metal clusters [10]. The greater tendency for the $(\eta^5$-$C_5(CH_3)_5Rh$ group to form rhodium–rhodium bonds than the $(\eta^5$-$C_5H_5)Rh$ group is probably responsible for the difference in product distribution observed in previous studies [10,21,22,23] and the low yield of cluster IV obtained in this study.

The major products in the absence of added H_2 are clusters which contain an $RhOs_2$ or $RhOs_3$ metal core. MOs_3 (M = Fe, Co, Ni) clusters were the principal products for reaction of $(\mu$-$H)_2Os_3(CO)_{10}$ with the first row metal carbonyls [1–4]. The yields of $(\eta^5$-$C_5H_5)RhOs_2(CO)_9$ (I) and $(\mu$-$H)_2(\eta^5$-$C_5H_5)RhOs_5(CO)_{10}$ (II) were comparable and account for more than 85% of the reaction products. The pentanuclear cluster, $(\mu$-$H)_2(\eta^5$-$C_5H_5)RhOs_4(CO)_{13}$ (III) was obtained in low yield. No trinuclear clusters with MOs_2 cores were observed in the products of any of the previous reactions of $(\mu$-$H)_2Os_3(CO)_{10}$ with metal carbonyls [1–4,6–12] and cluster I was not found when added H_2 was present. When H_2 was bubbled through a solution of cluster I (reaction 2a, Scheme 1) in toluene at 90 °C, $(\mu$-$H)_2(\eta^5$-$C_5H_5)_2Rh_2Os_2(CO)_7$ (IV) was produced in low yield. In addition, some of cluster II was also produced. This explains the absence of cluster I when added H_2 was present and suggests that cluster IV may result from reaction of cluster I with H_2.

$(\mu$-$H)_2(\eta^5$-$C_5H_5)RhOs_3(CO)_{10}$ (II). The molecular structure of compound II is shown in Fig. 1. Positional parameters, selected bond distances, and selected bond angles are given in Tables 2, 6, and 7, respectively. This structure is consistent with the structure in solution proposed from ^1H and ^{13}C NMR spectra at −60 °C [5]. It consists of an $RhOs_3$ tetrahedral metal core in which each osmium atom is linked to three terminal carbonyls. The rhodium atom is bound to the three osmium atoms, an η^5-C_5H_5 ligand and an asymmetric bridging carbonyl which spans the Rh–Os(2) atoms (Rh–C(1) 1.90(1) Å, Os(2)–C(1) 2.226(9) Å). As indicated in our earlier report of the proposed structure of II, the absence of any coupling of the hydride with ^{103}Rh in the ^1H NMR spectrum indicates that the hydrides must bridge Os–Os bonds [5a]. Although the positions of the two hydrogens were not determined

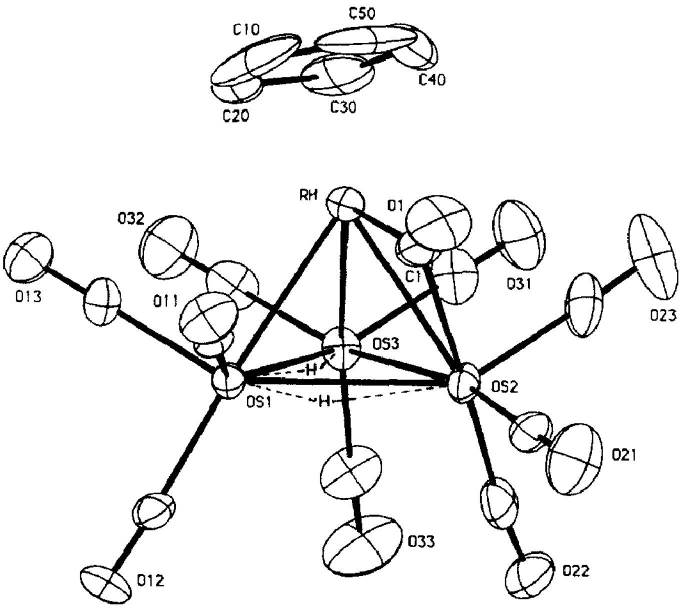

Fig. 1. Molecular structure of $(\mu\text{-H})_2(\eta^5\text{-C}_5H_5)RhOs_3(CO)_{10}$.

directly from the X-ray data, they are inferred as edge bridging between Os(1)–Os(2) and Os(1)–Os(3). The distances Os(1)–Os(2) 2.950(1) Å and Os(1)–Os(3) 2.867(1) Å are significantly longer than the remaining osmium-osmium bond in the cluster (Os(2)–Os(3) 2.782(1) Å). These osmium–osmium distances correspond very well with those observed in the related clusters $(\mu\text{-H})_2(\eta^5\text{-C}_5(CH_3)_5)RhOs_3(CO)_{10}$ [10] and $(\mu\text{-H})_2(\eta^5\text{-C}_5H_5)CoOs_3(CO)_{10}$ [1] which have molecular structures very similar to that of II. Rhodium–osmium distances are relatively uniform Os(1)–Rh 2.730(1) Å, Os(2)–Rh 2.736(1) Å and Os(3)–Rh 2.720(1) Å; they correspond well with the rhodium–osmium distances observed in $(\mu\text{-H})_2(\eta^5\text{-C}_5(CH_3)_5)RhOs_3(CO)_{10}$ [10]. The dihedral angle between the cyclopentadienide ring and the three osmium atoms is 24.0°.

$(\mu\text{-H})_2(\eta^5\text{-C}_5H_5)RhOs_4(CO)_{13}$ (III). The molecular structure of III is shown in Fig. 2. Positional parameters, selected bond distances, and bond angles are given in Tables 3, 8, and 9. The cluster consists of an Os_4 tetrahedral core with an Os–Os edge which is bridged by an $Rh(\eta^5\text{-C}_5H_5)(CO)$ unit. This is only the second example of a pentanuclear cluster and the first heteronuclear cluster with this core geometry. Osmium–osmium bond distances in cluster III compare well with those reported for the pentanuclear, homonuclear analogue $(\mu\text{-H})_2Os_5(CO)_{16}$ [24]. Each Os atom is bound to three terminal carbonyls. Bridge hydrogens were located. They span Os(1)–Os(4) and Os(2)–Os(4) with respective metal–metal distances of 2.954(1) and 2.941(1) Å, the longest osmium–osmium distances in the structure. The osmiums which are bridged by rhodium have the shortest metal–metal distance in the structure (Os(1)–Os(2) 2.758(1) Å). The dihedral angle between the Os(1)–Os(2)–Os(3) and Rh(1)–Os(1)–Os(2) planes is 3.6° and the angle between Os(1)–Os(2)–Os(4) and Rh(1)–Os(1)–Os(2) is 117.1°.

The proton NMR spectrum of cluster III is consistent with the reported structure. At 25°C in $CDCl_3$ the singlet of intensity 5 (6.05 ppm) is assigned to the

Table 2

Positional parameters and their estimated standard deviations of $(\mu\text{-H})_2(\eta^5\text{-C}_5H_5)RhOs_3(CO)_{10}$

Atom	x	y	z	B (Å^2) [b]
Os1	0.48440(6)	0.32057(4)	0.69724(3)	1.584(9)
Os2	0.23601(6)	0.34521(4)	0.56419(3)	1.847(9)
Os3	0.52064(6)	0.24743(4)	0.53580(3)	1.94(1)
Rh	0.2906(1)	0.18392(8)	0.63974(6)	1.87(2)
C1	0.118(2)	0.265(1)	0.6621(9)	2.6(3)
O1	0.001(1)	0.276(1)	0.7038(8)	4.3(3)
C11	0.346(2)	0.333(1)	0.7901(8)	1.9(2)
C12	0.625(2)	0.420(1)	0.7274(8)	2.2(3)
C13	0.620(2)	0.232(1)	0.7516(8)	2.4(3)
C21	0.071(2)	0.431(1)	0.5920(9)	2.6(3)
C22	0.340(2)	0.418(1)	0.4835(9)	3.0(3)
C23	0.104(2)	0.283(2)	0.4847(9)	3.5(4)
C31	0.419(2)	0.182(1)	0.447(1)	3.3(4)
C32	0.687(2)	0.159(1)	0.554(1)	3.0(3)
C33	0.655(2)	0.320(1)	0.468(1)	3.5(3)
O11	0.258(2)	0.3429(9)	0.8433(7)	3.5(3)
O12	0.711(2)	0.4749(6)	0.7479(7)	3.5(2)
O13	0.698(2)	0.1815(9)	0.7831(8)	3.8(3)
O21	−0.031(2)	0.481(1)	0.6062(9)	5.0(3)
O22	−0.388(2)	0.5363(9)	0.5672(7)	3.8(3)
O23	0.029(2)	0.243(1)	0.4375(9)	5.8(4)
O31	0.362(2)	0.144(1)	0.3957(8)	4.7(3)
O32	0.782(2)	0.106(1)	0.5653(9)	4.9(3)
O33	0.726(2)	0.364(1)	0.4261(8)	5.7(3)
C10	0.277(4)	0.072(1)	0.728(1)	6.8(7)
C20	0.408(3)	0.058(1)	0.677(1)	4.4(4)
C30	0.341(3)	0.043(1)	0.596(1)	4.4(5)
C40	0.177(2)	0.052(2)	0.601(1)	5.0(5)
C50	0.135(3)	0.072(1)	0.678(2)	6.8(5)
H10 [a]	0.284	0.077	0.788	7.8
H20 [a]	0.526	0.056	0.690	5.4
H30 [a]	0.395	0.029	0.547	5.4
H40 [a]	0.099	0.047	0.553	6.0
H50 [a]	0.021	0.084	0.692	7.8

[a] Positions calculated. [b] Anisotropically refined atoms are given in the form of the isotropic equivalent thermal parameter defined as: $(4/3)[a^2\beta_{1,1} + b^2\beta_{2,2} + c^2\beta_{3,3} + ab(\cos\gamma)\beta_{1,2} + ac(\cos\beta)\beta_{1,3} + bc(\cos\alpha)\beta_{2,3}]$.

η^5-C_5H_5 and the sharp singlet of intensity 2 (−18.24 ppm) is assigned to the equivalent bridging hydrogens.

$(\mu\text{-H})_2(\eta^5\text{-C}_5H_5)_2Rh_2Os_2(CO)_7$ (IV). The molecular structure of cluster IV is shown in Fig. 3. Positional parameters and selected bond distances and bond angles are given in Tables 4, 10, and 11. This cluster consists of an Rh_2Os_2 tetrahedral unit in which each osmium atom is bound to three terminal carbonyls and each rhodium is bound to a C_5H_5 ring. A bridging carbonyl spans the Rh atoms. Positions of hydrogen atoms were not determined, but the presence of Os(1)–H–Os(2) and Os(1)–H–Rh(3) bridges are inferred by the metal–metal distances Os(1)–Os(2) 2.822(1) Å and Os(1)–Rh(3) 2.899(1) Å, which are significantly longer than the other metal–metal distances in the molecule. The dihedral angle between the

C(31)–C(32)–C(33)–C(34)–C(35) plane and the Os(1)–Os(2)–Rh(4) plane is 25.9° and the dihedral angle between the C(41)–C(42)–C(43)–C(44)–C(45) and the Os(1)–Os(2)–Rh(3) plane is 21.1°. The dihedral angle between the two cyclopentadienyl rings is 52.5°. The structure of IV closely resembles that of $(\mu\text{-H})_2(\eta^5\text{-}$

Table 3

Positional parameters and their estimated standard deviations of $(\mu\text{-H})_2(\eta^5\text{-C}_5H_5)\text{RhOs}_4(\text{CO})_{13}$

Atom	x	y	z	B (Å^2) [a]
Os1	0.16247(4)	0.12287(3)	0.14846(3)	1.960(9)
Os2	0.25406(4)	0.11051(3)	0.35706(3)	1.796(8)
Os3	0.41126(4)	0.06199(3)	0.24524(4)	1.966(9)
Os4	0.37892(4)	0.22652(2)	0.26314(4)	1.876(8)
Rh1	0.00409(9)	0.16176(6)	0.25692(8)	2.68(2)
O1	0.075(1)	0.3354(6)	0.266(1)	5.6(3)
O11	−0.046(1)	0.4565(6)	0.3834(8)	4.1(2)
O12	0.258(1)	0.1017(8)	−0.0283(7)	5.1(3)
O13	−0.069(1)	0.2072(7)	−0.0024(9)	4.9(3)
O21	0.5094(8)	0.0863(5)	0.5271(6)	2.9(2)
O22	0.152(1)	0.1611(7)	0.5220(8)	5.1(3)
O23	0.166(1)	−0.0616(5)	0.3640(8)	4.2(2)
O31	0.5389(9)	0.0600(6)	0.0853(7)	3.7(2)
O32	0.6722(8)	0.0345(6)	0.4040(7)	3.7(2)
O33	−0.345(1)	0.1160(6)	−0.223(1)	5.2(3)
O41	−0.3599(9)	0.2643(6)	−0.0691(8)	4.1(2)
O42	0.328(1)	0.4057(5)	0.2704(8)	4.6(3)
O43	0.491(1)	0.2460(6)	0.0942(8)	4.3(2)
C1	0.057(1)	0.2686(8)	0.264(1)	3.6(3)
C11	0.088(1)	0.0207(7)	0.1312(9)	2.3(2)
C12	0.230(1)	0.1075(8)	0.0404(9)	2.9(3)
C13	0.014(1)	0.1754(8)	0.057(1)	3.2(3)
C21	0.417(1)	0.0923(7)	0.4616(9)	2.3(2)
C22	0.181(1)	0.1450(8)	0.456(1)	3.1(3)
C23	0.197(1)	0.0039(7)	0.359(1)	2.9(3)
C31	0.492(1)	0.0608(7)	0.1462(9)	2.8(3)
C32	0.573(1)	0.0454(7)	0.3408(9)	2.4(2)
C33	0.366(1)	−0.0494(7)	0.2317(9)	2.5(3)
C41	0.541(1)	0.2310(7)	0.367(1)	3.0(3)
C42	0.343(1)	0.3385(7)	0.2690(9)	2.3(2)
C43	0.451(1)	0.2388(8)	0.158(1)	3.3(3)
C10	−0.164(1)	0.090(1)	0.170(2)	7.6(5)
C20	−0.204(2)	0.166(1)	0.183(2)	6.4(5)
C30	−0.176(1)	0.180)	0.286(1)	5.2(4)
C40	−0.117(1)	0.114(1)	0.335(2)	8.3(6)
C50	−0.113(1)	0.054(1)	0.257(2)	11.5(9)
H1	0.30(1)	0.211(8)	0.36(1)	4.0
H2	0.22(1)	0.220(8)	0.17(1)	4.0
H10	−0.170	0.066	0.104	5.7
H20	−0.243	0.205	0.129	5.5
H30	−0.195	0.227	0.319	5.0
H40	−0.078	0.103	0.407	5.7
H50	−0.083	−0.001	0.270	6.7

[a] Anisotropically refined atoms are given in the form of the isotropic equivalent thermal parameter defined as: $(4/3)[a^2\beta_{1,1} + b^2\beta_{2,2} + c^2\beta_{3,3} + ab(\cos\gamma)\beta_{1,2} + ac(\cos\beta)\beta_{1,3} + bc(\cos\alpha)\beta_{2,3}]$.

Table 4

Positional parameters and their estimated standard deviations of $(\mu\text{-H})_2(\eta^5\text{-C}_5H_5)_2Rh_2Os_2(CO)_7$

Atom	x	y	z	B (Å^2) [a]
Os1	0.11606(4)	0.02569(2)	0.31301(2)	2.358(6)
Os2	0.09068(4)	−0.14739(2)	0.26304(2)	2.608(6)
Rh3	0.36977(8)	−0.10096(4)	0.35996(4)	2.23(1)
Rh4	0.30082(8)	−0.04267(4)	0.19842(4)	2.22(1)
O	0.5940(9)	0.0295(5)	0.3032(5)	4.7(2)
O11	−0.141(1)	0.0838(5)	0.1704(5)	4.8(2)
O12	0.325(1)	0.1860(5)	0.3024(6)	5.7(2)
O13	0.057(1)	−0.0920(6)	0.5411(5)	7.6(2)
O21	−0.195(1)	−0.1469(6)	0.1204(7)	7.8(3)
O22	0.273(1)	−0.2857(4)	0.1784(5)	5.2(2)
O23	−0.054(1)	−0.2657(5)	0.3880(6)	5.6(2)
C	0.478(1)	−0.0137(6)	0.2898(5)	2.8(2)
C11	−0.048(1)	0.0624(5)	0.2210(6)	3.3(2)
C12	0.246(1)	0.1264(6)	0.3065(6)	3.2(2)
C13	0.005(1)	0.0667(6)	0.4049(7)	4.1(2)
C21	−0.089(1)	−0.1485(7)	0.1757(8)	4.9(3)
C22	0.207(1)	−0.2338(5)	0.2105(6)	3.2(2)
C23	0.000(1)	−0.2218(6)	0.3388(7)	3.9(2)
C31	0.416(1)	−0.2353(6)	0.4034(8)	4.9(2)
C32	0.560(1)	−0.2006(8)	0.3782(7)	5.8(2)
C33	0.609(1)	−0.1355(8)	0.4356(9)	6.7(3)
C34	0.492(2)	−0.1283(8)	0.4889(8)	7.4(3)
C35	0.378(1)	−0.1865(8)	0.4716(7)	6.3(2)
C41	0.397(1)	−0.0976(7)	0.0793(6)	3.9(2)
C42	0.462(1)	−0.0168(8)	0.0970(6)	4.7(2)
C43	0.338(2)	0.0459(7)	0.0917(6)	5.2(3)
C44	0.189(2)	0.0004(8)	0.0726(6)	4.9(2)
C45	0.224(2)	−0.0853(3)	0.0613(3)	5.2(3)
H31	0.3564	−0.2837	0.3777	7.0
H32	0.6137	−0.2191	0.3304	7.0
H33	0.7072	−0.1003	0.4365	7.0
H34	0.4901	−0.0868	0.5349	7.0
H35	0.2805	−0.1950	0.5003	7.0
H41	0.4563	−0.1508	0.0785	7.0
H42	0.5786	−0.0047	0.1112	7.0
H43	0.3519	0.1060	0.0991	7.0
H44	0.0816	0.0261	0.0681	7.0
H45	0.1423	−0.1292	0.0450	7.0

[a] Anisotropically refined atoms are given in the form of the isotropic equivalent thermal parameter defined as: $(4/3)\,[a^2\beta_{1,1} + b^2\beta_{2,2} + c^2\beta_{3,3} + ab(\cos\gamma)\beta_{1,2} + ac(\cos\beta)\beta_{1,3} + bc(\cos\alpha)\beta_{2,3}]$.

$C_5(CH_3)_5)_2Rh_2Os_2CO_7$ [10] including the proposed arrangement of the bridging hydrogens.

Additional evidence for the positions of the hydrogen atoms in IV is provided by the proton NMR spectrum at −60 °C in $CDCl_3$. A singlet of intensity 1 (−15.40 ppm) is assigned to the bridging hydrogen along the Os–Os bond, while a doublet of intensity 1 (−20.03 ppm, *J*(Rh–H) 30.7 Hz) is assigned to the bridging hydrogen along the Rh–Os bond. As the temperature is raised the signals begin to merge to give one peak of intensity 2 (−11.09 ppm). This is consistent with the previously

(continued on p. 436)

Table 5

Positional parameters and their estimated standard deviations of $(\mu\text{-H})_3(\eta^6\text{-C}_6\text{H}_6)\text{RhOs}_3(\text{CO})_9$

Atom	x	y	z	B (Å^2) [a]
Os	0.13359(2)	0.06681(2)	0.15816(1)	1.901(5)
Rh	0.000	0.000	0.28578(5)	2.416(9)
O1	0.2761(4)	0.1379(5)	0.0084(3)	4.0(1)
O2	0.2517(5)	0.2820(5)	0.2427(4)	4.8(1)
O3	0.2514(4)	−0.0309(4)	0.2428(4)	4.7(1)
C1	0.2188(5)	0.1091(5)	0.0628(4)	2.6(1)
C2	0.2096(5)	0.2023(5)	0.2107(4)	2.9(1)
C3	0.2093(5)	0.0080(5)	0.2109(4)	3.0(1)
C4	−0.1131(8)	−0.056(1)	0.3926(6)	6.9(4)
C5	0.1118(3)	0.055(1)	0.3903(6)	7.1(4)
H4	−0.1905	−0.0941	0.3943	7.5
H5	0.1892	0.0939	0.3874	8.5

[a] Anisotropically refined atoms are given in the form of the isotropic equivalent thermal parameter defined as: $(4/3)[a^2\beta_{1,1} + b^2\beta_{2,2} + c^2\beta_{3,3} + ab(\cos\gamma)\beta_{1,2} + ac(\cos\beta)\beta_{1,3} + bc(\cos\alpha)\beta_{2,3}]$.

Table 6

Interatomic distances (Å) and esd's for $(\mu\text{-H})_2(\eta^5\text{-C}_5\text{H}_5)\text{RhOs}_3(\text{CO})_{10}$

(A) Metal–metal distances			
Os(1)–Os(2)	2.950(1)	Os(1)–Rh	2.730(1)
Os(1)–Os(3)	2.867(1)	Os(2)–Rh	2.736(1)
Os(2)–Os(3)	2.782(1)	Os(3)–Rh	2.729(1)
(B) Carbonyl distances			
Rh–C(1)	1.90(1)	C(1)–O(1)	1.19(1)
(C) Metal–ring distances			
Rh–C(10)	2.21(1)	Rh–C(20)	2.19(1)
Rh–C(30)	2.26(1)	Rh–C(40)	2.25(1)
Rh–C(50)	2.19(1)		

Table 7

Bond angles (deg) and esd's for $(\mu\text{-H})_2(\eta^5\text{-C}_5\text{H}_5)\text{RhOs}_3(\text{CO})_{10}$

(A) *Metal angles*			
Os(1)–Os(2)–Os(3)	59.95(1)	Os(2)–Os(3)–Os(1)	62.93(1)
Os(1)–Os(2)–Rh	57.24(2)	Os(2)–Os(1)–Os(3)	57.12(1)
Os(1)–Rh–Os(3)	63.49(2)	Os(2)–Os(1)–Rh	57.44(2)
Os(1)–Rh–Os(2)	65.32(2)	Os(2)–Os(3)–Rh	59.63(2)
Os(1)–Os(3)–Rh	58.43(2)	Os(3)–Rh–Os(2)	61.31(2)
Rh–Os(1)–Os(3)	58.08(2)	Rh–Os(2)–Os(3)	59.06(2)
(B) Metal–carbonyl angles			
Rh–C(1)–O(1)	143.1(9)	Os(2)–C(1)–O(1)	134.2(8)
Os(1)–Rh–C(1)	83.0(3)	Os(1)–Os(2)–C(1)	73.0(3)
Os(2)–Rh–C(1)	53.8(3)	Os(3)–Os(2)–C(1)	102.1(3)
Os(3)–Rh–C(1)	114.7(3)		

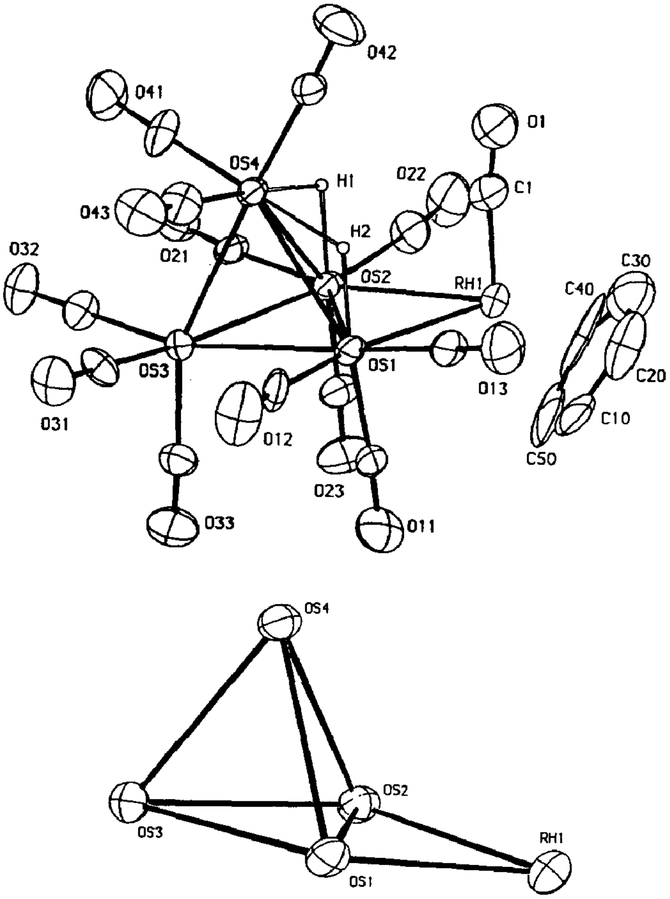

Fig. 2. Molecular structure of $(\mu\text{-H})_2(\eta^5\text{-C}_5H_5)RhOs_4(CO)_{13}$.

Table 8

Interatomic distances (Å) and esd's for $(\mu\text{-H})_2(\eta^5\text{-C}_5H_5)RhOs_4(CO)_{13}$

(A) Metal – metal distances			
Rh(1)-Os(1)	2.770(1)	Rh(1)-O(2)	2.789(1)
Os(1)-Os(2)	2.758(1)	Os(1)-Os(3)	2.824(1)
Os(1)-Os(4)	2.954(1)	Os(2)-Os(3)	2.837(1)
Os(2)-Os(4)	2.941(1)	Os(3)-Os(4)	2.876(1)
(B) Carbonyl distances			
Rh(1)-C(1)	1.87(1)	C(1)-O(1)	1.13(1)
(C) Metal – ring distances			
Rh(1)-C(10)	2.20(1)	Rh(1)-C(20)	2.19(1)
Rh(1)-C(30)	2.19(1)	Rh(1)-C(40)	2.15(2)
Rh(1)-C(50)	2.21(2)		
(D) Metal – hydride distances			
Os(1)-H(2)	1.7(1)	Os(2)-H(1)	1.7(1)
Os(4)-H(1)	1.8(1)	Os(4)-H(2)	1.8(1)

Table 9

Bond angles (deg) and esd's for $(\mu\text{-H})_2(\eta^5\text{-C}_5H_5)RhOs_4(CO)_{13}$

(A) Metal angles			
Os(1)–Rh(1)–Os(2)	59.20(2)	Rh(1)–Os(2)–Os(1)	59.92(2)
Rh(1)–Os(1)–Os(2)	60.58(2)	Os(1)–Os(4)–Os(3)	58.85(1)
Os(1)–Os(4)–Os(2)	55.80(1)	Os(1)–Os(3)–Os(4)	63.55(1)
Os(1)–Os(3)–Os(2)	58.32(1)	Os(1)–Os(2)–Os(4)	62.34(1)
Os(1)–Os(2)–Os(3)	60.60(1)	Os(2)–Os(1)–Os(4)	61.86(1)
Os(2)–Os(1)–Os(3)	61.08(1)		
(B) Metal – carbonyl angles			
Os(1)–Rh(1)–C(1)	90.3(4)	Rh(1)–C(1)–O(1)	172(1)
Os(2)–Rh(1)–C(1)	91.2(3)		

reported structure of the pentamethylcyclopentadienyl analogue. $(\mu\text{-H})_2(\eta^5\text{-C}_5(CH_3)_5)_2Rh_2Os_2(CO)_7$ [10].

$(\mu\text{-H})_4(\eta^5\text{-C}_5H_5)RhOs_3(CO)_9$ (V). The proposed structure of compound V is shown in Fig. 4. This structure is based on ^{1}H NMR and IR spectral comparisons with the known structure of the pentamethylcyclopentadienyl analogue, $(\mu\text{-H})_4(\eta^5\text{-C}_5(CH_3)_5)RhOs_3(CO)_9$ [10]. Figure 4 displays the IR spectrum of V and the related clusters $(\mu\text{-H})_4(\eta^5\text{-C}_5H_5)CoOs_3(CO)_9$ and $(\mu\text{-H})_4(\eta^5\text{-C}_5(CH_3)_5)RhOs_3(CO)_9$. The metal hydride region of the ^{1}H NMR spectrum of V at −80 °C in CD_2Cl_2 consists of a doublet of intensity 2 (−18.13 ppm (J(Rh–H) 25 Hz)) assigned to the hydrogens bridging the Rh–Os bonds and a singlet of intensity 2 (−19.47 ppm) assigned to the hydrogens bridging the Os–Os bonds. A signal of intensity 5 (5.71

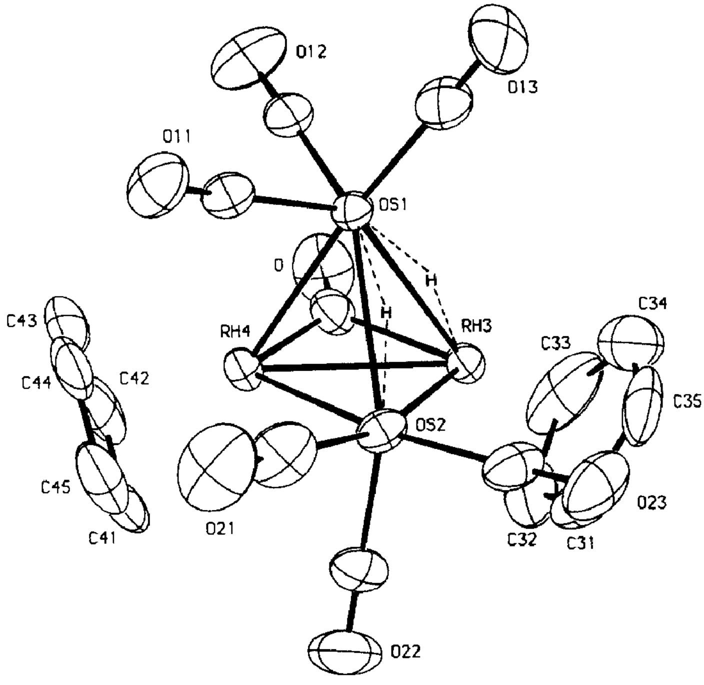

Fig. 3. Molecular structure of $(\mu\text{-H})_2(\eta^5\text{-C}_5H_5)_2Rh_2Os_2(CO)_7$.

Table 10

Interatomic distances (Å) and esd's for $(\mu\text{-H})_2(\eta^5\text{-C}_5H_5)_2Rh_2Os_2(CO)_7$

(A) Metal-metal distances			
Os(1)-Os(2)	2.822(1)	Os(2)-Rh(3)	2.680(1)
Os(1)-Rh(3)	2.899(1)	Os(2)-Rh(4)	2.670(1)
Os(1)-Rh(4)	2.716(1)	Rh(3)-Rh(4)	2.691(1)
(B) Metal-ring distances			
Rh(3)-C(31)	2.229(8)	Rh(4)-C(41)	2.290(7)
Rh(3)-C(32)	2.196(8)	Rh(4)-C(42)	2.235(7)
Rh(3)-C(33)	2.227(9)	Rh(4)-C(43)	2.229(8)
Rh(3)-C(34)	2.186(10)	Rh(4)-C(44)	2.178(8)
Rh(3)-C(35)	2.204(8)	Rh(4)-C(45)	2.268(8)
(C) Metal-carbonyl distances			
Rh(3)-C	2.029(7)	Rh(4)-C	1.958(7)

Table 11

Bond angles (deg) and esd's for $(\mu\text{-H})_2(\eta^5\text{-C}_5H_5)_2Rh_2Os_2(CO)_7$

(A) Metal angles			
Os(2)-Os(1)-Os(3)	55.87(1)	Os(1)-Os(2)-Rh(3)	63.52(1)
Os(2)-Os(1)-Rh(4)	57.61(1)	Os(1)-Os(2)-Rh(4)	59.21(1)
Rh(3)-Os(1)-Rh(4)	57.16(1)	Rh(3)-Os(2)-Rh(4)	60.39(1)
Os(1)-Rh(3)-Os(2)	60.62(1)	Os(1)-Rh(4)-Os(2)	63.18(1)
Os(1)-Rh(3)-Rh(4)	58.01(2)	Os(1)-Rh(4)-Rh(3)	64.83(2)
Os(2)-Rh(3)-Rh(4)	59.61(2)	Os(2)-Rh(4)-Rh(3)	60.00(2)
(B) Metal-carbonyl angles			
Os(1)-Rh(3)-C	75.4(2)	Os(1)-Rh(4)-C	81.0(2)
Os(2)-Rh(3)-C	105.8(2)	Os(2)-Rh(4)-C	108.4(2)
Rh(4)-Rh(3)-C	46.4(2)	Rh(3)-Rh(4)-C	48.7(2)
Rh(3)-C-O	134.0(6)	Rh(4)-C-O	141.1(6)

ppm) is assigned to the $(\eta^5\text{-C}_5H_5)$ ligand. The ^{1}H NMR spectrum closely resembles that of the analogues $(\mu\text{-H})_4(\eta^5\text{-C}_5H_5)CoOs_3(CO)_9$ [3] and $(\mu\text{-H})_4(\eta^5\text{-C}_5(CH_3)_5)RhOs_3(CO)_9$ [10].

$(\mu\text{-H})_3(\eta^6\text{-C}_6H_6)RhOs_3(CO)_9$ (VII). The molecular structure of compound VII is shown in Fig. 5. Positional parameters, selected bond distances, and bond angles are given in Tables 5, 12 and 13. C_3 symmetry is crystallographically imposed on the molecule which has C_{3v} point symmetry. The structure contains an $RhOs_3$ tetrahedral core, the bond distances for which are in excellent agreement with those in

Table 12

Interatomic distances (Å) and esd's for $(\mu\text{-H})_3(\eta^6\text{-C}_6H_6)RhOs_3(CO)_9$

(A) Metal-metal distances			
Os-Os	2.887(1)	Os-Rh	2.701(1)
(B) Metal-ring distances			
Rh-C(4)	2.271(8)	Rh-C(5)	2.230(8)

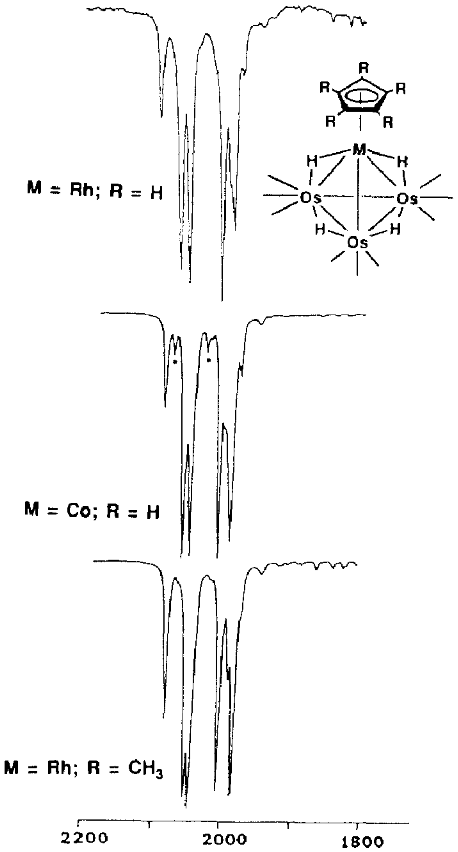

Fig. 4. IR spectra of $(\mu\text{-H})_4(\eta^5\text{-C}_5\text{H}_5)\text{RhOs}_3(\text{CO})_9$, $(\mu\text{-H})_4(\eta^5\text{-C}_5\text{H}_5)\text{CoOs}_3(\text{CO})_9$, and $(\mu\text{-H})_4(\eta^5\text{-C}_5(\text{CH}_3)_5)\text{RhOs}_3(\text{CO})_9$. * Asterisk denotes two strong peaks due to $(\mu\text{-H})_4\text{Os}_4(\text{CO})_{12}$ impurity.

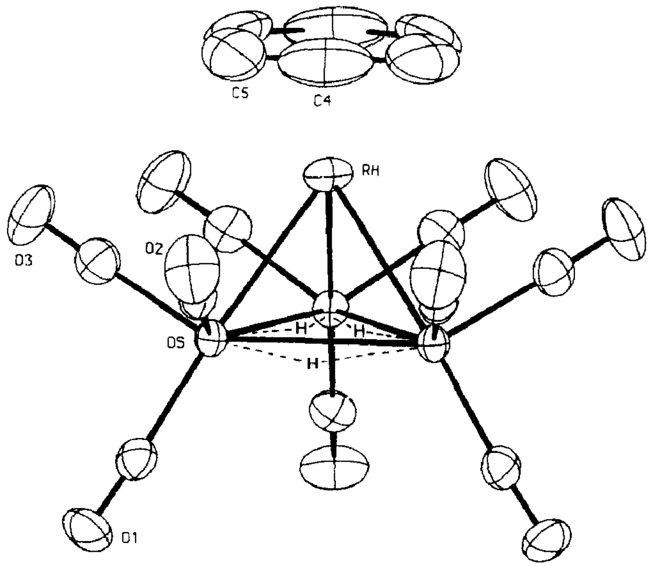

Fig. 5. Molecular structure of $(\mu\text{-H})_3(\eta^6\text{-C}_6\text{H}_6)\text{RhOs}_3(\text{CO})_9$.

Table 13

Bond angles (deg) and esd's for $(\mu\text{-H})_3(\eta^6\text{-C}_6H_6)RhOs_3(CO)_9$

(A) Metal angles			
Os–Os–Os	60.00(1)	Os–Os–Rh	57.69(1)
Os–Rh–Os	64.62(1)		
(B) Metal–carbonyl angles			
Os–Os–C(1)	118.9(2)	Os–Os–C(2)	93.6(2)
Os–Os–C(3)	142.9(2)		

the related complex $(\mu\text{-H})_3(\eta^6\text{-C}_6H_5CH_3)RhOs_3(CO)_9$ (VI) [6]. Three terminal carbonyls are bound to each osmium atom and the benzene ring is bound to the rhodium atom. Based upon the long Os–Os distances (Os–Os' = Os–Os' = Os'–Os'' = 2.887(1) Å) and the absence of spin-coupling between bridge protons and ^{103}Rh in the ^{1}H NMR spectrum, the H atoms are believed to bridge adjacent osmium atoms. The ^{1}H NMR spectrum in acetone-d_6 at −60 °C contains a signal of intensity 3 (−17.43 ppm), which is assigned to the three bridge atoms. A low field signal of intensity 6 (6.68 ppm) is assigned to the benzene hydrogen. These assignments are consistent with the previously reported structure of $(\mu\text{-H})_3(\eta^6\text{-C}_6H_5CH_3)RhOs_3(CO)_9$ (VI) [10].

Summary

The reaction of $(\mu\text{-H})_2Os_3(CO)_{10}$ with $(\eta^5\text{-C}_5H_5)Rh(CO)_2$ in toluene in the absence of added H_2 favors the formation of the trinuclear and tetranuclear clusters $(\eta^5\text{-C}_5H_5)RhOs_2(CO)_9$ and $(\mu\text{-H})_2(\eta^5\text{-C}_5H_5)RhOs_3(CO)_{10}$ in about equal yields (ca. 40%). A minor product is $(\mu\text{-H})_2(\eta^5\text{-C}_5H_5)RhOs_4(CO)_{13}$ (3.5% yield), a pentanuclear cluster with a tetrahedral $RhOs_3$ core that is Os–Os edge bridged by a $Rh(\eta^5\text{-C}_5H_5)(CO)$ group. This is the first example of a pentanuclear heteronuclear cluster shown to contain an edge-bridged metal atom and only the second pentanuclear cluster of this shape. On the other hand in the presence of added H_2 the cluster $(\mu\text{-H})_3(\eta^6\text{-C}_6H_5CH_3)RhOs_3(CO)_9$ is the principal product (25% yield). It appears that hydrogen reacts oxidatively with the starting material, $(\eta^5\text{-C}_5H_5)Rh(CO)_2$, and then reduces the cyclopentadienyl group which then may be eliminated as cyclopentadiene or cyclopentane with addition of an arene solvent molecule to the rhodium. Minor products formed are $(\mu\text{-H})_2(\eta^5\text{-C}_5H_5)RhOs_3(CO)_{10}$ (8% yield) and $(\mu\text{-H})_2(\eta^5\text{-C}_5H_5)_2Rh_2Os_2(CO)_7$ (7% yield). When the reaction is carried out in benzene in the presence of added H_2 the cyclopentadienyl ligand is replaced by the benzene and $(\mu\text{-H})_3(\eta^6\text{-C}_6H_6)RhOs_3(CO)_9$ is produced (10% yield).

There is a marked difference between the reactions cited above and the previously reported reactions with $(\eta^5\text{-C}_5(CH_3)_5)Rh(CO)_2$ under equivalent conditions. In the absence of H_2 the principal product is $(\eta^5\text{-C}_5(CH_3)_5)Rh_2Os_2(CO)_8$ (35% yield); $(\mu\text{-H})_2(\eta^5\text{-C}_5(CH_3)_5)Rh_2Os_2(CO)_7$ is the main product (36% yield) in the presence of added H_2.

Supplementary material. A complete list of observed bond distances and bond angles and calculated structure factor amplitudes is available upon request from the National Auxilliary Publications Service (NAPS). See NAPS document no. 04719 for 149 pages of supplementary material. Order from NAPS c/o Microfiche Publications, P.O. Box 3515, Grand Centeral Station, New York, New York 10163-3513. Remit with your order, not under separate cover, \$46.45 (U.S. funds on a U.S. Bank only) for photocopies or \$4.00 for microfiche. Outside the U.S. and Canada, add postage of \$4.50 for the first 20 pages and \$1.00 for each additional 10 pages of material thereafter, \$1.50 for microfiche postage. Institutions and Organizations may order by purchase order. However, there is a billing and handling charge for this service of \$15, plus any applicable postage.

Acknowledgements

We thank the National Science Foundation for support of this work through Grant CHE 88-00515 and Grant CHE 84-11630 for an X-ray diffractometer. NMR spectra were obtained at The Ohio State University Campus Chemical Instrument Center (funded in part by NSF Grant 79-10019 and NIH Grant 1 S10 PRO145128-01A). A.C. was supported in part by a NATO Postdoctoral Fellowship.

References

1 J.S. Churchill, C. Bueno, S. Kennedy, J.C. Bricker, S.G. Shore, Inorg. Chem., 21 (1982) 627.
2 J.S. Plotkin, D.G.S. Alway, C.R. Weisenberger, S.G. Shore, J. Am. Chem. Soc., 102 (1980) 6156.
3 (a) S.G. Shore, W.-L. Hsu, C.R. Weisenberger, M.L. Caste, M.R. Churchill, C. Bueno, Organometallics, 1 (1982) 1405; (b) M. Castiglioni, E. Sappa, M. Valle, M. Langfranchi, A. Tiripicchio, J. Organomet. Chem., 241 (1983) 99.
4 M.R. Churchill, C. Bueno, W.-L. Hsu, J.S. Plotkin, S.G. Shore, Inorg. Chem., 21 (1982) 1958.
5 (a) L.-Y. Hsu, W.-L. Hsu, D.-Y. Jan, A.G. Marshall, S.G. Shore, Organometallics, 3 (1984) 591; (b) D.-Y. Jan, L.-Y. Hsu, W.-L. Hsu, A. Colombie, S.G. Shore, Abstr. Papers, 193rd Nat. Meeting Am. Chem. Soc., Annaheim, Ca. American Chemical Society, Washington, D.C., 1986.
6 S.G. Shore, W.-L. Hsu, M.R. Churchill, C. Bueno, J. Am. Chem. Soc., 105 (1983) 655.
7 Stone and coworkers have developed a general method for the preparation of mixed-metal clusters from the reactions of platinum metal-olefin complexes. (a) L.J. Farrugia, J.A.K. Howard, P. Mitprachachon, J.L. Spencer, F.G.A. Stone, P.J. Woodward, J. Chem. Soc., Chem. Comm., (1978) 260; (b) L.J. Farrugia, J.A.K. Howard, P. Mitrpachachon, F.G.A. Stone, P. Woodward, J. Chem. Soc., Dalton (1981) 171; (c) B.F.G. Johnson, J. Lewis, P.R. Raithby, S.N. Zsman, B. Syed-Mustaffa, W.J. Taylor, K.H. Whitmire, W. Clegg, J. Chem. Soc., Dalton, (1984) 2111.
8 E.W. Burkhardt, G.L. Goeffroy, J. Organomet. Chem., 198 (1980) 179.
9 P. Sundberg, N. Bertil, B.F.G. Johnson, J. Lewis, P.R. Raithby, J. Organomet. Chem., 353 (1988) 383.
10 D.-Y. Jan, L.-Y. Hsu, W.-L. Hsu, S.G. Shore, Organometallics, 6 (1987) 274.
11 L.-Y. Hsu, W.-L. Hsu, D.-Y. Jan, S.G. Shore, Organometallics, 5 (1986) 1049.
12 M.R. Churchill, C. Bueno, J. Organomet. Chem., 256 (1983) 357.
13 W.E. Lindsell, C.B. Knobler, H.D. Kaesz, J. Organomet. Chem., 296 (1985) 209.
14 D.F. Shriver, M.A. Drezdzon, The Manipulation of Air-Sensitive Compounds; 2nd edit., Wiley-Interscience, New York, 1986.
15 S.A.R. Knox, J.W. Koepke, M.A. Andrews, H.D. Kaesz, J. Am. Chem. Soc., 97 (1975) 3942.
16 W. Hieber, H.Z. Legally, Z. Anorg. Allgem. Chem., 96 (1943) 251.
17 SDP (Structure Determination Package; B.A. Frenz and Associates, College Station, Tx., 1982.
18 E.O. Fischer, K. Bittler, Z. Naturforschg. B, 16 (1961) 225.
19 E.O. Fischer, H. Wawersik, J. Organomet. Chem., 5 (1966) 559; E.O. Fischer, O.S. Mills, E.F. Pauleis, H. Wawersik, Chem. Comm., (1967) 643.
20 M. Panaque, P.M. Maitlis, J. Chem. Soc., Chem. Commun., 105 (1989).
21 J. Plank, D. Riedel, W.A. Hermann, Angew. Chem., Int. Ed. Engl., 19 (1980) 937.
22 A. Nulton, P.M. Maitlis, J. Organomet. Chem., 166 (1979) C21.
23 R.J. Lawson, J.R. Shapley, J. Am. Chem. Soc., 98 (1976) 7433.
24 J.J. Guy, G.M. Sheldrick, Acta Crystallogr., 34 (1978) 1725.